



HAL
open science

Semidiurnal and diurnal tidal effects in the middle atmosphere as seen by Rayleigh lidar

Sarah Gille, Alain Hauchecorne, Marie-Lise Chanin

► **To cite this version:**

Sarah Gille, Alain Hauchecorne, Marie-Lise Chanin. Semidiurnal and diurnal tidal effects in the middle atmosphere as seen by Rayleigh lidar. *Journal of Geophysical Research: Atmospheres*, 1991, 96 (D4), pp.7579-7587. 10.1029/90JD02570 . insu-03598672

HAL Id: insu-03598672

<https://insu.hal.science/insu-03598672>

Submitted on 5 Mar 2022

HAL is a multi-disciplinary open access archive for the deposit and dissemination of scientific research documents, whether they are published or not. The documents may come from teaching and research institutions in France or abroad, or from public or private research centers.

L'archive ouverte pluridisciplinaire **HAL**, est destinée au dépôt et à la diffusion de documents scientifiques de niveau recherche, publiés ou non, émanant des établissements d'enseignement et de recherche français ou étrangers, des laboratoires publics ou privés.

Copyright

Semidiurnal and Diurnal Tidal Effects in the Middle Atmosphere as Seen by Rayleigh Lidar

SARAH T. GILLE,¹ ALAIN HAUCHECORNE, AND MARIE-LISE CHANIN

Service d'Aéronomie du Centre National de la Recherche Scientifique, Verrières-le-Buisson, France

The Rayleigh lidar at the Centre d'Essais des Landes has been adjusted to provide continuous day and nighttime measurements when clear weather permits with high resolution in both time and space. These measurements are processed to show tidal effects in the 30- to 80-km height range. The observed temperature variations in two 11-day series of data, from November 1988 and January 1989, are treated by spectral analysis and by least squares fitting sinusoids for 12- and 24-hour periods. The observed tidal amplitudes correspond with experimental results from rocket studies and are generally consistent, though somewhat larger than predicted in theoretical models. Observed lidar phases are roughly corroborated by radar observations and also follow the same general trends as model predictions.

1. INTRODUCTION

Laser temperature soundings of the atmosphere, obtained by Rayleigh lidar, have been performed on an ongoing basis at night, whenever clear weather permits at the Observatory of Haute-Provence, France (44°N, 6°E), since 1981 and at the Centre d'Essais des Landes (CEL), Biscarrosse, France (44°N, 1°W), since 1986 [Hauchecorne and Chanin, 1980; Chanin, 1984; Chanin and Hauchecorne, 1984]. Lidar data, providing absolute temperature information in the 30- to 80-km altitude range, have been used extensively in studies of gravity wave effects [Wilson, 1989] and long-term temperature trends [Chanin *et al.*, 1987]. Until recently, however, long continuous data sets suitable for analysis of medium-frequency effects, such as tidal fluctuations, were not available from lidars.

Instead, in the past decade, observational studies of solar atmospheric tides have relied primarily on radar wind measurement techniques, which give detailed wind velocity profiles from the surface up to 30 km and above 80-km altitude, though certain sites measure from altitudes as low as 60 km. Radar data sets have permitted thorough analysis of semidiurnal and diurnal tidal amplitudes and phases and, in particular, have shown the rapid changes in tidal patterns which occur around the equinoxes [e.g., Manson *et al.*, 1988; Tsuda *et al.*, 1988; Vincent *et al.*, 1988].

However, between 30- and 60-km altitude, where lidar operates but radar is blind, determination of tidal effects has proved more elusive. Tidal studies in this range have thus far been limited almost exclusively to a series of rocket temperature and wind studies carried out in the 1960s. Many of these rocket campaigns were conducted over periods of time too short to clearly distinguish the cyclical tidal effects from short-term gravity wave induced fluctuations. While rocket wind measurements have demonstrated the general trends of semidiurnal and diurnal tidal effects [Groves, 1980], temperature measurements are more limited, and it is only by combining all available rocket data that valuable measures of

diurnal tidal effects have been obtained [Hoxit and Henry, 1973.] More recently, Hitchman and Leovy [1985] examined 3 months of limb infrared monitor of the stratosphere (LIMS) satellite day-night temperature differences at the equator to obtain an idea of tidal temperature amplitudes in the 30- to 60-km range. Their results put lower limits on the diurnal amplitude; but the nature of LIMS data, which provides only two measurements a day, near noon and midnight, renders complete separation of tidal phase and amplitude impossible.

Recent modifications to the lidar at CEL have extended operating hours, thus making lidar measurements available as an additional means to study tidal effects between 30 and 80 km. In September 1988 the system was automated, so that on clear nights it now runs continuously, using detectors to trigger a shutdown in case of sudden cloud cover, rain, or fire. Two months later, in November, the frequency response was fine-tuned to reduce background effects, permitting daytime operation.

In the first 7 months since daytime measurements began, two periods of clear weather, in November 1988 and in the latter half of January 1989, provided extended series of temperature profiles sufficient for analysis for tidal effects. This paper discusses the adjustments made to permit daytime measurements, then describes the treatment and analysis of the November and January data sets, and compares the results with previous experiments and model results for the semidiurnal and diurnal solar tide.

2. DAYTIME MEASUREMENTS

Daytime lidar measurements were previously impossible because the background light from the sun overpowered the returned laser signal. Three improvements were made in order to reduce this background. First, since emission and reception are coaxial in the CEL system, it was possible to cut the field of view of the telescope in half to 1×10^{-4} rad. Second, an intracavity Fabry-Perot filter was installed in the laser to narrow the emission line to 3 pm. Third, a Fabry-Perot filter with a full width at half maximum of 10 pm was added to the interference filter at the receiving end and tuned to coincide with the emission wavelength. With these adjustments, background light is now about equal to the laser echo at 40 km and may be measured and removed.

¹Now at MIT-WHOI Joint Program, Massachusetts Institute of Technology, Cambridge.

Copyright 1991 by the American Geophysical Union.

Paper number 90JD02570.
0148-0227/91/90JD-02570\$05.00

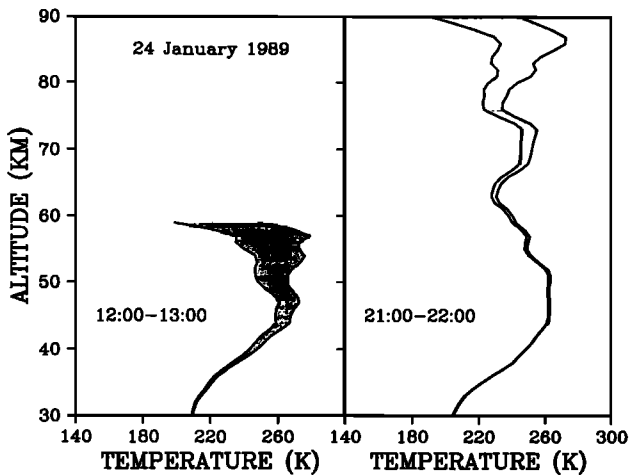


Fig. 1. Typical day and night integrated hourly temperature profiles from January 24, 1989. (Left) Daytime temperature with $\pm\sigma$ error bars from 1200 to 1300 UT (almost exactly local time). (Right) Nighttime temperature and error bars from 2100 to 2200 UT.

The lidar control system records both daytime and nighttime measurements at 3-min integrated density profiles with 300-m vertical resolution. Raw data are converted to temperature assuming hydrostatic equilibrium and the ideal gas law and, for this study, are averaged to yield hourly temperature slices, thus increasing the altitude range and smoothing out high-frequency fluctuations. Data points are vertically smoothed using a 17-point discrete prolate spheroidal filter [Mathews *et al.*, 1983] in order to remove small gravity wave effects and are then adjusted to give a uniform one data point per kilometer vertical distribution.

Figure 1 shows typical 1-hour averages for daytime and nighttime temperature measurements. Statistically determined density error bars are propagated through all the calculations; when density error bars are greater than 15% of the measured density, temperature values are discarded. While nighttime measurements normally stretch from 30 to 90 km, daytime data typically reach their upper limits between 55 and 60 km. In both cases, error bars are less than 1°K at the lower limits and climb rapidly to 10° or 20°K in the upper 4 or 5 km.

3. ANALYSIS

Radar work has suggested that tidal effects should be studied using roughly 10-day data series since shorter intervals may show nonglobal effects [Forbes, 1985] and longer periods may be contaminated with seasonal migration of the tidal phase and magnitude [Manson *et al.*, 1988]. For convenience, we selected 11-day periods of data for analysis, using 71 hours of nighttime data and 28 hours of daytime data taken from November 14 to 25, 1988, and 102 nighttime hours plus 25 daytime hours from January 20 to 31, 1989.

Seven consecutive nights in January, each with a minimum of 12 hours of data, provide a first-order approximation of winter tidal trends. Plate 1 shows the 7-night hourly average temperatures with altitudinal means removed. Although daytime weather during the same week was not consistent enough to justify inclusion of daytime data in the treatment, the series is nonetheless helpful in illustrating the mean tidal effects. While the results represent a mixture of

semidiurnal and diurnal processes, clearly visible warm and cold temperature bands suggest a strong tidal effect with a descending phase and a vertical wavelength of roughly 30 km.

Rarely, however, does the weather permit such an extended set of nighttime data as the January series in Plate 1, and even less often are meteorological conditions clear continuously for 24 hours. During times of clear weather, occasional cloud cover typically limits measurements to about half the hours within the time period. Thus analysis techniques chosen must correctly process data series with frequent gaps.

3.1. Spectral Analysis

Ferraz-Mello [1981] has developed a method to perform a spectral analysis of a time series of unequally spaced observations by means of a data-compensated discrete Fourier transform. Plate 2 shows the amplitude response of this transform performed on the January daytime and nighttime data for periods ranging from around 60 hours down to about 6 hours at each kilometer altitude. Amplitude response is particularly strong at 12 hours (corresponding to a frequency of 0.0831 h^{-1}) and at 24 hours (0.0416 h^{-1}) above 50 km. This suggests that for the January data, semidiurnal and diurnal tidal effects dominate gravity wave responses for periods between 10 and 60 hours in the mesosphere. Test spectral analyses were performed on artificial data consisting of white noise with the same distribution in time as the actual data and superimposed with a sinusoidal tidal effect varying with altitude. The resulting artificial spectra show that in agreement with the spectrum shown in Plate 2, the spectral analysis of the data should not show any clear tidal effect below about 50 km. The same analyses performed on artificial white noise alone without a tidal signal indicate that the distribution of the data should not create any spurious spectral signals. The apparent split of the tidal signal below 50 km into two peaks corresponding to 20- and 30-hour periods, with a trough between them at 24 hours, thus appears to be a real effect which might be attributed to a resonance of phase fluctuations or higher-frequency gravity waves.

As Plate 3 shows, tidal effects in the spectral analysis are much less pronounced in November. Spectral analysis tests on white noise series distributed in the same pattern as the November data predict noisier results, particularly at low altitudes and low frequencies, with a weaker tidal signal than the January analysis. While it is difficult to draw conclusions from the limited quantity of data now available, two other factors should be considered. First, as radar studies of equinoctial phase changes have shown, tides undergo significant and rapid changes from summer to winter conditions as late as the end of November [Tsuda *et al.*, 1988], during which time semidiurnal tidal amplitudes are significantly reduced. Although our data series represents a different altitude range and does not begin until November 14, it may still be subject to some rapid equinoctial transitions. Any phase changes or amplitude reductions during this period would diminish the magnitude of the spectral response for the critical diurnal and semidiurnal frequencies in November. Second, Wilson [1989] has shown that while November and January gravity wave activities are typically roughly equivalent between 30 and 60 km, above 60 km at CEL,

gravity waves are significantly more active in November than in January. This increased activity at higher altitudes, where tidal effects would be expected to appear stronger, may mean that a broad spectrum of gravity wave frequencies partially resists filtering and drowns out the apparent tidal effects in November.

3.2. Least Squares Fitting

Although the spectral analysis discussed above gives a very clear qualitative notion of tidal responses, it does not facilitate removal of linear trends, simultaneous determination of 12- and 24-hour effects in cases where the interaction between the two may be deceptive, or error propagation to obtain an idea of the statistical validity of the results. Thus in order to quantify the measures of tidal response, the same two series of data were fit with a linear combination of 12- and 24-hour sine and cosine waves, plus a constant value and a linear effect using the singular value decomposition method described by *Press et al.* [1986]. From the calculated sine and cosine amplitudes an amplitude and phase shift were determined.

Background signal is assumed to be a constant level of white noise at all frequencies. It is found at each altitude by performing a spectral analysis for high frequencies, corresponding to periods between 2 and 5 hours, represented as frequencies 0.5–0.2 in Figure 2. The average of the amplitudes in this frequency range, shown in Figure 3, is removed from the semidiurnal and diurnal amplitudes found using the singular value decomposition method. Figures 4–7 show the resulting tidal amplitudes and phases for November and January. By convention, tidal phase is depicted as the time of maximum amplitude.

Tsuda et al. [1987] have shown that error bars, which vary systematically over the course of the day, may result in an imbalance in the weighting of the data and, as a result, a poor tidal fit. Since lidar error bars are generally larger during the day than at night, for this study they are fixed at a minimum value of 2°K to prevent insignificant variations in error bars from causing enormous differences in the weights and skewing the results. Tests show that tidal amplitudes and phases found by averaging all 11 days of data into 24 one hour slices before fitting fall within the error bars of the results shown in the figures. In addition, values found using the data's statistical error bars as weighting factors (thus significantly reducing the importance of the daytime data to the fitting routines) also generally fall well within the error bars of the printed results.

One of the problems in fitting unevenly distributed data is determining how much the inability of the curve fitter to work around the gaps may contribute to the error in the final results. *Lindzen and Chapman* [1969] probed this question and concluded that if the tidal effect is not the dominant signal, spurious noise may contribute more to the experimental amplitudes than the tide itself. *Crary and Forbes* [1983] investigated the expected error bars for tidal effects fit to noisy measurements distributed over only one part of the day by fitting diurnal and semidiurnal tidal effects to white noise series of lengths varying from 6 to 18 hours. We repeated their numerical tests, extending the white noise series to have the same distribution as our 11-day series, with the standard deviation of the white noise set equivalent to the statistical error bars. Results indicated that error bars

generated by the curve-fitting package correctly estimate the standard deviation of the difference between the tidal amplitude due to white noise and the true amplitude (zero, in the case of white noise).

Above 60 km the tidal fit is more difficult to perform, partly because fewer data points are available to fit six functions (diurnal sine and cosine, semidiurnal sine and cosine, a constant, and a linear trend) but primarily because all of the data are concentrated in the same 12- to 14-hour period each night. Since the measurements are relatively noisy, the singular value decomposition cannot clearly distinguish half a diurnal sine wave from a full semidiurnal wave; and in a worst case scenario, such as the hypothetical data depicted in Figure 8, if only 12 hours of noisy measurements are available each day, the two effects may be effectively identical. While the pair of functions is not entirely degenerate, the result is much the same: the tidal amplitude grows excessively large as the computer searches for the best fit. To alleviate this problem, we investigated the possibility of finding the diurnal and semidiurnal effects separately by calling the fitting subroutines once for the 24-hour period and a second time for the 12-hour period. Expanding on *Crary and Forbes'* [1983] method, we generated noisy diurnal and semidiurnal sine waves, using a variety of relative phases and varying the signal to noise ratio. Results indicate that separate fits for diurnal and semidiurnal effects are more accurate for a signal to noise ratio of 5, if there are fewer than 9 hours of data per day; for a signal to noise ratio of 3, if there are fewer than 11 hours of data; and for a signal to noise ratio of 1, if there are fewer than 16 hours of data. Thus in our particular case, up to about 60 km, the combined fit poses few problems since the signal to noise ratio is rarely much worse than 1, and the data cover most of the daytime hours. Above 60 km, however, the maximum number of hours per day drops to 13 in January and 14 in November, while the signal to noise ratio is consistently less than 3 (with the exception of two or three points in high-amplitude peaks between 60 and 70 km, which we ignore to insure continuity in the final results). Thus, using the criteria determined by the white noise tests as a guideline, above 60 km, we fit the semidiurnal and diurnal tidal effects separately. A side effect of this fitting procedure is that the variance of the fit parameters (as determined by the curve-fitting package) underestimates the true uncertainty in the parameters, because it is determined as if only four functions are used rather than six. Error bars shown on the plots are instead derived from the standard deviation of amplitude and phase errors in repeated statistical tests performed on artificial data.

Resulting tidal diurnal amplitudes (Figures 4 and 6) vary from as low as $0.5^\circ \pm 0.5^\circ\text{C}$ around 30-km altitude to values roughly between about 1° and $12^\circ \pm 6^\circ\text{C}$ above 60 km. Semidiurnal amplitudes (Figures 5 and 7) range from about $0.6^\circ \pm 0.4^\circ\text{C}$ around 30 km to between 1° and $8^\circ \pm 4^\circ\text{C}$ above 60 km. November diurnal phases have wavelengths around 10 km below 50-km elevation and around 100 km from 65 to 80 km (Figure 4). January diurnal phases (Figure 6) have a wavelength of roughly 30 km from 45 to 70 km and about 100 km from 35 to 45 km. November semidiurnal phases (Figure 5) have wavelengths of approximately 15 km below 45-km altitude and around 35 km from 60- to 80-km altitude. In January (Figure 7), semidiurnal phase wavelengths are near

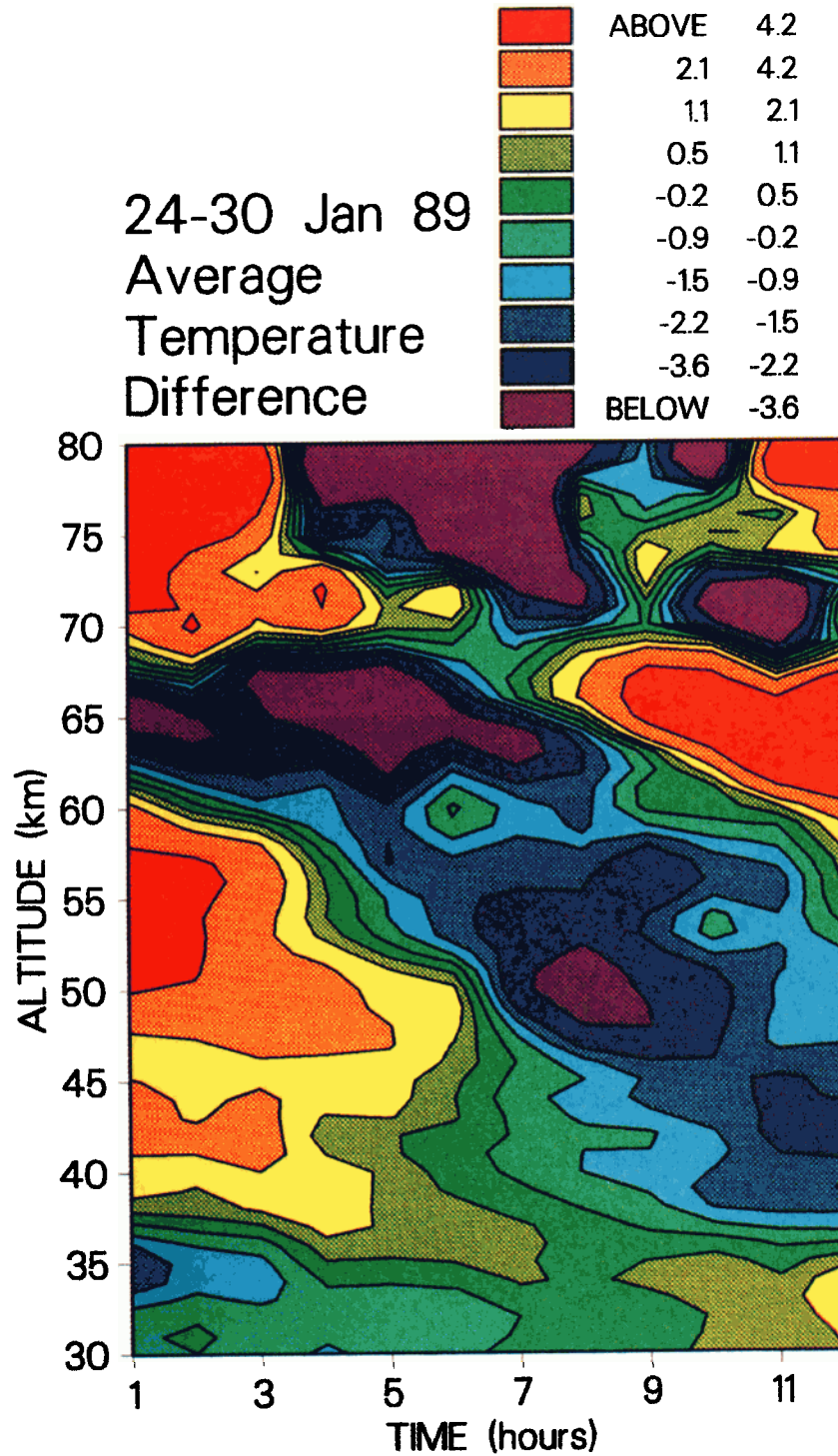


Plate 1. Hourly temperatures averaged over seven nights, with the mean temperature at each kilometer altitude subtracted out. Blue- and purple-colored regions show cooler temperatures descending in altitude over the course of the night, with a vertical wavelength of roughly 30 km.

infinite from 30 to 55 km and are around 35 km from 55 to 70 km.

4. RESULTS AND COMPARISONS

4.1. Radar and Rocket Studies

Most recent observational tidal studies have made use of radar wind data from about 60 to 110 km. While wind

amplitudes and phase maxima would not be expected to correlate with temperature amplitudes and phases, the vertical wavelength for the phase should be roughly consistent in the 60- to 80-km range where lidar and radar data overlap, though radar data are somewhat limited in this range and the lidar measurements have substantial error bars. Measurements at the Saskatoon radar site (52°N, 107°W) from 1981 to 1985 show January semidiurnal wavelengths to be 35–45 km,

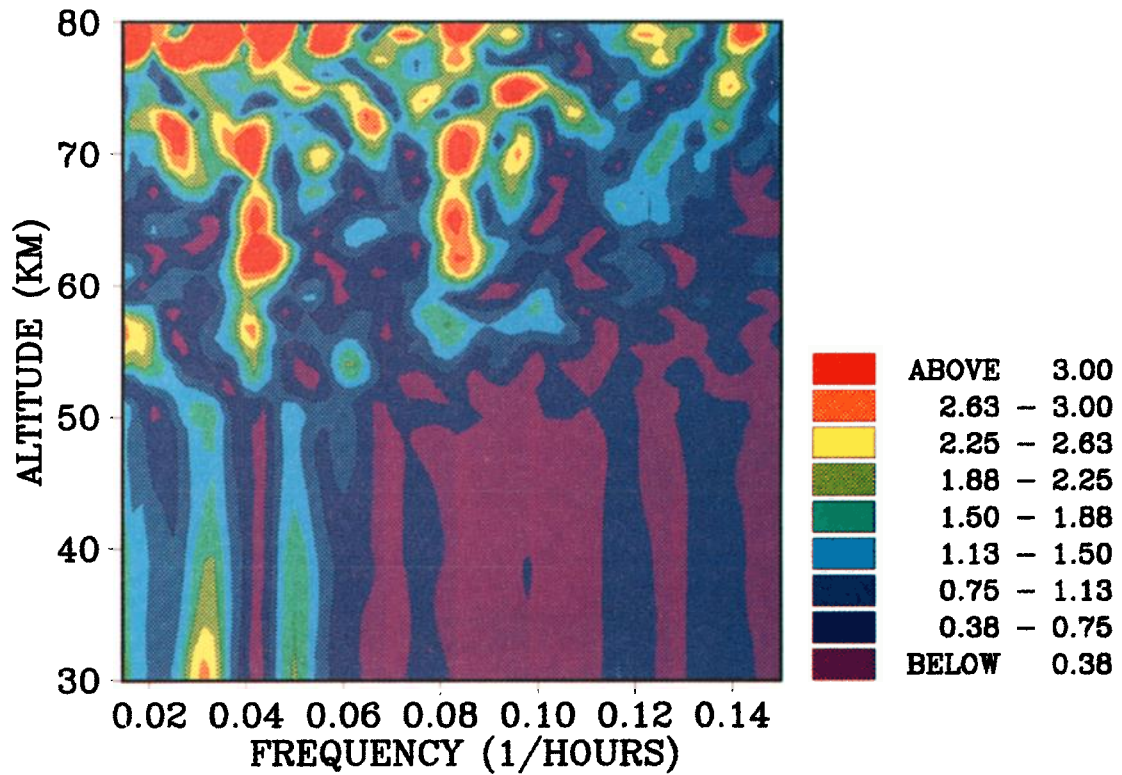


Plate 2. Spectral analysis for data taken from January 20 to 31, 1989. Red, orange, and yellow regions show strong amplitudes, most notably at 0.0831 and 0.0416 h^{-1} , corresponding to 12 and 24 hours, respectively.

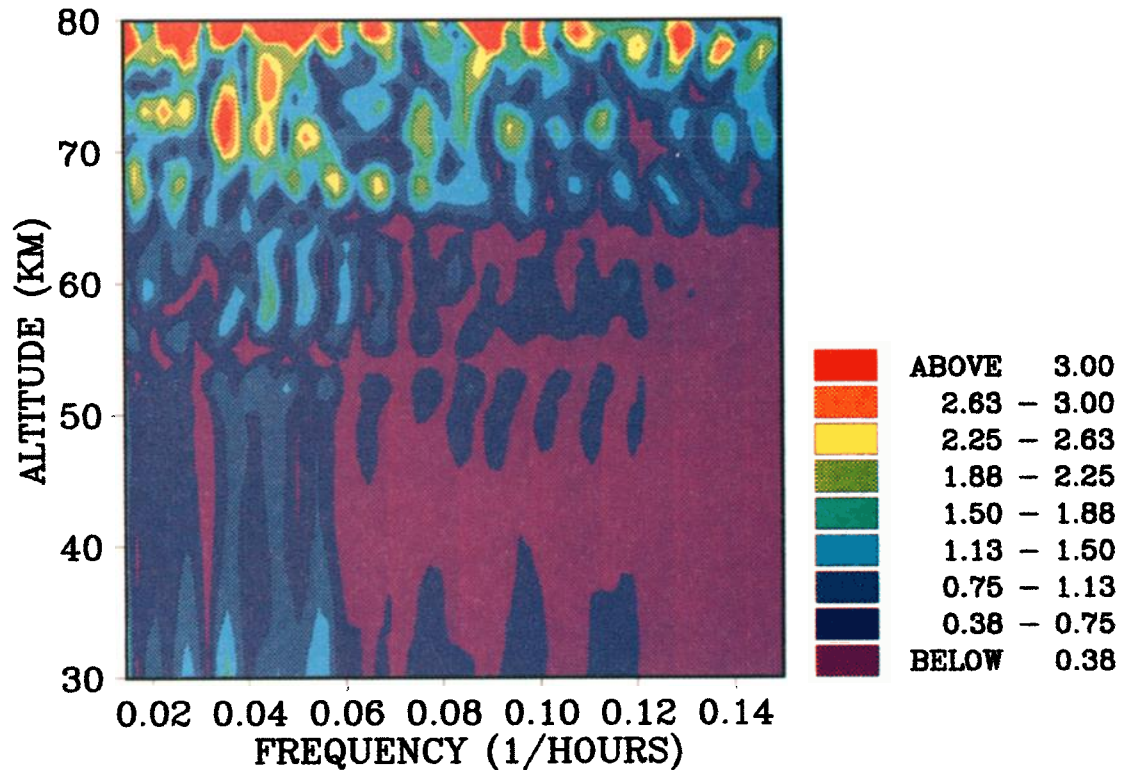


Plate 3. Spectral analysis for data taken from November 14 to 23, 1988, with same scale as Plate 2.

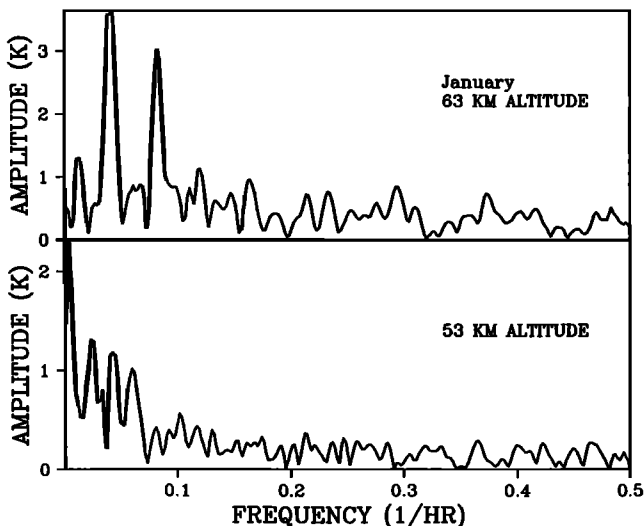


Fig. 2. Spectral analyses at 53 and 63 km, respectively. The range between 0.2 and 0.5 h^{-1} (5–2 hours) is averaged and removed from the calculated signal as noise.

though in this altitude range, wavelengths may occasionally be much longer or ill defined [Manson and Meek, 1986; Tsuda et al., 1988; Manson et al., 1988, 1989]. These values correspond roughly with the 40-km wavelength observed from 60 to 70 km and much longer wavelength above 70 km (Figure 7). The same studies also show that November is a month of strong phase transitions, separating the summer state when wavelengths are approximately 50 km and the winter state. By the end of November, when lidar measurements were taken, radar wavelengths in the overlap altitude range are typically 30–40 km, roughly corresponding to the 30-km wavelength in lidar observations above 60 km (Figure 5). Radar data show phase differences from 1 to 3 hours between November and January; lidar temperature data appear to show more significant phase differences, as much as 6 hours, which may simply indicate that temperature and wind respond differently to seasonal changes or which may stem from the large error bars in high-altitude lidar measurements. Radar studies show that diurnal phases in the 60-

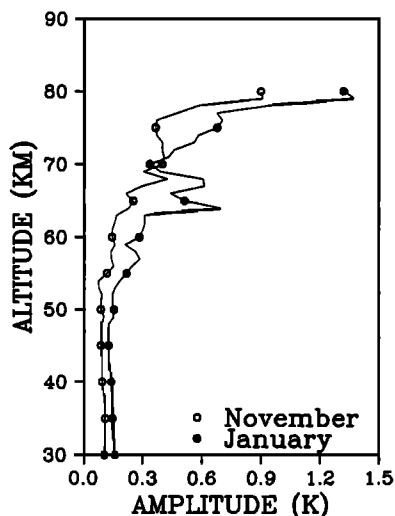


Fig. 3. Average white noise for January and November data.

80-km range are frequently irregular or evanescent, making comparison more difficult, although the 20- to 80-km wavelengths in lidar data appear reasonable.

Previous middle atmosphere tidal studies using mid-latitude temperature data are limited almost exclusively to Hoxit and Henry [1973], who compiled rocket data gathered between 1964 and 1969 at White Sands (32.5°N), Cape Kennedy (28.5°N), and Wallops Island (37.8°N), sorting it into 10 daytime and 10 nighttime slots to obtain an average tidal amplitude for middle latitudes. Though their results should be regarded cautiously because limited data prevented consideration of seasonal and latitudinal variations and because a number of systematic problems plagued the rocket instrumentation, their work is one of very few mid-latitude, tidal temperature studies in the 30- to 80-km range. They found average diurnal temperature variation corre-

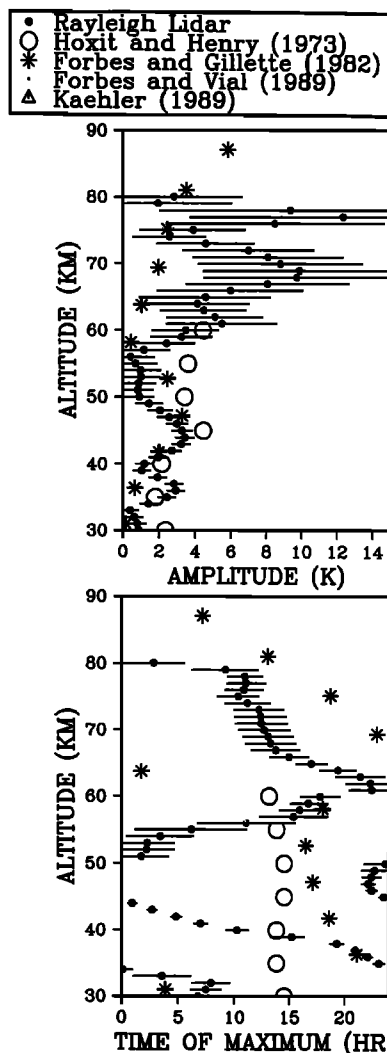


Fig. 4. Height profiles of temperature diurnal phases (time of maximum amplitude) and amplitudes observed from November 14 to 23, 1988 (solid circles with error bars added), superposed with model results (asterisks) from Forbes and Gillette [1982] and with rocket measurements (open circles) from Hoxit and Henry [1973]. Error bars for Hoxit and Henry's results are roughly $\pm 2^\circ\text{K}$. The reader is cautioned about the uncertainties in lidar-derived tidal harmonics above 60 km, where only nighttime data are available. See text for details.

sponding to amplitudes of 2.35°, 1.80°, 2.15°, 4.45°, 3.40°, 3.60°, and 4.45°K at 30, 35, 40, 45, 50, 55, and 60 km, respectively. As Figures 4 and 6 indicate, the tidal amplitudes provided by lidar for both the months of January and November do not differ substantially in magnitude from the results of Hoxit and Henry.

Hoxit and Henry's [1973] diurnal phase is roughly constant at about 1400 UT for all altitudes; in contrast, as shown in Figures 4 and 6, the lidar results indicate that the diurnal phase is consistent with an upward propagating tide in January, but the reverse phase gradient in November suggests that there is tidal mode mixing or reflection. If, as radar studies suggest, tidal phases vary substantially throughout the year, the discrepancy between the constant phase observed in the rocket studies and the descending phases found in lidar measurements may be attributed to Hoxit and Henry's averaging process: if the phase at each altitude varies significantly over the course of a year, then we would expect Hoxit and Henry's annual average to be constant. These differences between the rocket and lidar phases

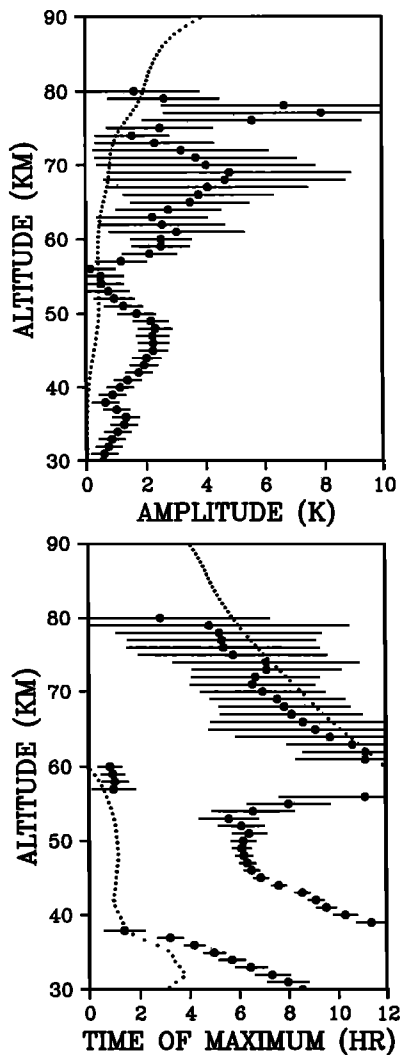


Fig. 5. Height profiles of November semidiurnal temperature phases and amplitudes, superposed with model results (small solid circles) from *Forbes and Vial* [1989].

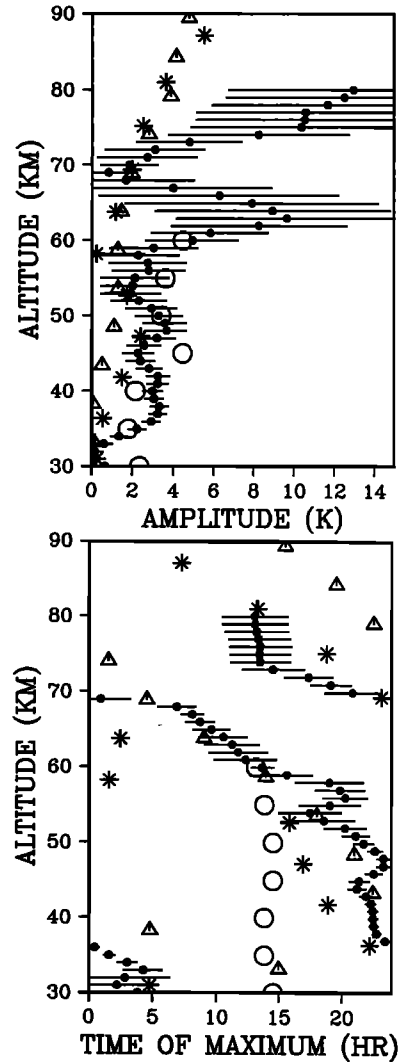


Fig. 6. Same as Figure 4 but for measurements from January 20 to 31, 1989. Triangles indicate winter solstice model results from *Kähler* [1989a]. Error bars for Kähler's phases are ± 45 min.

reinforce the idea that restraint should be exercised in interpreting any comparison of the results.

4.2. Model Predictions

Diurnal and semidiurnal tides have received considerable attention from modelers in recent years. While models tend not to account for atmospheric tidal effects such as local evanescent waves and interannual variability, comparison is nonetheless useful. *Kähler* [1989a] developed a three dimensional nonlinear tidal model based on primitive equations which has been run for winter solstice conditions, *Forbes and Gillette* [1982] modeled diurnal tidal effects for equinox and solstice conditions following the scheme discussed by *Forbes* [1982], and *Forbes and Vial* [1989] have refined a monthly two-dimensional linear semidiurnal tidal model, originally developed by *Vial* [1986]. Results from these three models have been superimposed on the lidar observations shown in Figures 4-7. (For the Forbes and Gillette results, a weighted mean of calculations at 42°N and 48°N is used. Winter solstice conditions are included with January data;

the Forbes and Gillette equinox conditions are shown with November diurnal data.) Model amplitudes increase with altitude, following the same general trends as the observed amplitudes. Diurnal results by *Forbes and Gillette* [1982] are consistent with observations up to 60 km (Figures 4 and 6), but semidiurnal amplitudes are significantly weaker than the data would suggest, matching observations only at the minima of 15 km vertical amplitude fluctuations (Figures 5 and 7). In part, the discrepancies may occur because phase fluctuations tend to flatten average seasonal and monthly tidal amplitudes relative to 10-day amplitudes, occasionally by as much as a factor of 3. Other factors which may add to the discrepancies between theory and measurement include observational problems, such as a poor signal to noise ratio, perhaps due to the strength of gravity waves, and effects not currently incorporated into the model equations, such as coupling between tidal forcing and either gravity waves [Walterscheid *et al.*, 1986] or planetary waves [Teitelbaum, 1989]. *Kähler* [1989b] has shown that variations in thermal forcing in the troposphere may produce substantially different temperature amplitudes in the middle atmosphere while having very little impact on the tidal phases. Finally, recent work by *Fraser et al.* [1989] indicates that interannual

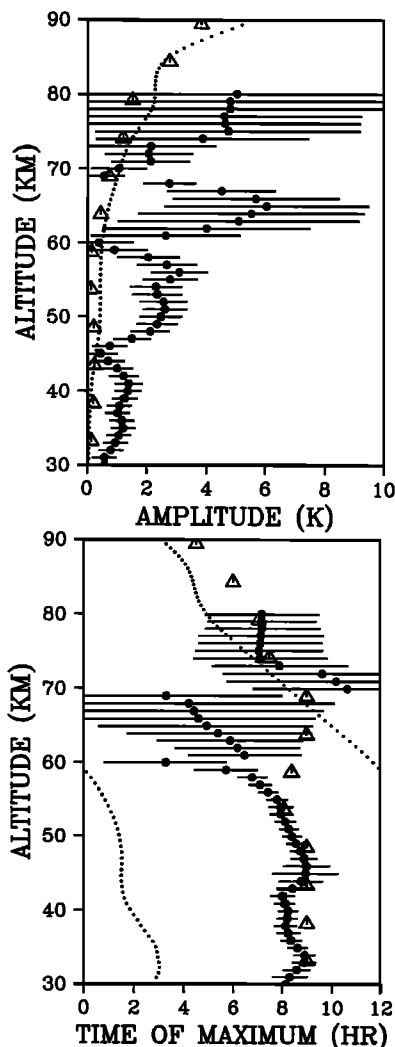


Fig. 7. Same as Figure 5 but for January values and with *Kähler* [1989a] and model results (triangles.)

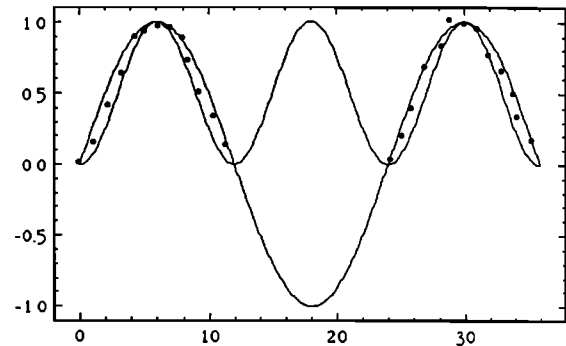


Fig. 8. Hypothetical hourly data points superimposed on diurnal and semidiurnal sine waves show that in the worst of cases, 12- and 24-hour effects may be effectively inseparable if only 12 hours of noisy data are available.

variability of tidal amplitudes may be as great as 50%, suggesting that it is difficult to estimate how representative data from one single year are.

Like amplitudes, observed and modeled phases are consistent to varying degrees. *Kähler's* [1989a] winter solstice model results (Figure 7) around 44°N show a descending diurnal phase closely matching that found in the January lidar data between 35 and 70 km, with a vertical wavelength of 35 km. *Kähler's* semidiurnal model phases, like the lidar results, are relatively stable at 0800 UT and decrease at higher altitudes, above 60 or 70 km. The *Forbes and Vial* [1989] semidiurnal model (Figure 7) shows a January phase which has values similar to the measured phases above 70 km, though slopes depart significantly, and follows the same trend as the measurements, though consistently shifted by about 6 hours below 70 km. The *Forbes-Vial* November results (Figure 5) closely match the lidar measurements above 55 km but do not follow the complicated observed phase changes at lower altitudes. *Forbes and Gillette* [1982] diurnal results follow the same general trend as the January observations (Figure 6), with occasional differences, notably between 58 and 65 km, and above 70 km where the model shows consistently short (60 km) wavelengths and the lidar appears to indicate a longer wavelength consistent with radar climatologies. Neither winter solstice nor equinox results exactly match the observed phase changes, though the general trends of descending phase above 60 km and a reverse gradient from 45 to 60 km are somewhat similar to equinox predictions.

5. SUMMARY AND CONCLUSION

This paper has examined tidal effects in two periods of lidar temperature data from November and January. While it would be difficult to justify drawing any sweeping conclusions from just two 11-day series of data, these initial results, at the very least, suggest that the Rayleigh temperature lidar may be a useful tool for deciphering tidal effects in the middle atmosphere. In general, it appears that temperature amplitudes correspond reasonably with rocket data results, and phase comparisons with radar climatologies are consistent. Some phases compare quite well with theoretical predictions, particularly January diurnal phases from 50 to 70 km, November semidiurnal from 55 to 80 km, and January semidiurnal below 60 km, but disagreements are often substantial below 60 km, where lidar results are most reliable.

Lidar-derived tidal amplitudes are in many cases significantly larger than model results would predict. The discrepancies between theoretical tidal predictions and those found by lidar and rocket studies may suggest that tidal effects involve more complicated processes than theory has thus far examined and, perhaps, couple with gravity waves or planetary waves to create greater amplitudes than previously anticipated. As more lidar data become available for tidal analysis, the current questions about phase, amplitude, and seasonal trends may eventually resolve themselves.

Acknowledgments. We are grateful to François Vial for helpful discussions and to Malte Kähler for generously providing us with unpublished model results. This study made use of the CEDAR Data Base at the National Center for Atmospheric Research in Boulder, Colorado, which is supported by the National Science Foundation. This research was supported by the Direction des Recherches, Etudes et Techniques under grant DRET88/188 and by the Centre National d'Etudes Spatiales under grant HPP/CNES/88/5219/00.

REFERENCES

- Chanin, M. L., Review of lidar contributions to the description and understanding of the middle atmosphere, *J. Atmos. Terr. Phys.*, **11**, 987–993, 1984.
- Chanin, M. L., and A. Hauchecorne, Lidar studies of temperature and density using Rayleigh scattering, *MAP Handb.* **13**, pp. 87–98, Univ. of Ill., Urbana, 1984.
- Chanin, M. L., N. Smires, and A. Hauchecorne, Long-term variation of the temperature of the middle atmosphere at mid-latitude: Dynamical and radiative causes, *J. Geophys. Res.*, **92**, 933–941, 1987.
- Crary, D. J., and J. M. Forbes, On the extraction of tidal measurements covering a fraction of a day, *Geophys. Res. Lett.*, **10**, 580–582, 1983.
- Ferraz-Mello, S., Estimation of periods from unequally spaced observations, *Astron. J.*, **86**, 619–624, 1981.
- Forbes, J. M., Atmospheric tides, 1, Model descriptions and results for the solar diurnal component, *J. Geophys. Res.*, **87**, 5222–5240, 1982.
- Forbes, J. M., Middle atmosphere tides, *MAP Handb.* **18**, pp. 50–56, Univ. of Ill., Urbana, 1985.
- Forbes, J. M., and D. F. Gillette, A compendium of theoretical atmospheric tidal structures, *AFGL Tech. Rep.*, *AFGL-TR-82-0173(I)*, 193 pp., 1982.
- Forbes, J. M., and F. Vial, Monthly simulations of the solar semidiurnal tide in the mesosphere and lower thermosphere, *J. Atmos. Terr. Phys.*, **51**, 649–661, 1989.
- Fraser, G. J., R. A. Vincent, A. H. Manson, C. E. Meek, and R. R. Clark, Interannual variability of tides in the mesosphere and lower thermosphere, *J. Atmos. Terr. Phys.*, **51**, 555–567, 1989.
- Groves, G. V., Seasonal and diurnal variations of middle atmosphere winds, *Philos. Trans. R. Soc. London, Ser. A*, **296**, 19–40, 1980.
- Hauchecorne, A., and M. L. Chanin, Density and temperature profiles obtained by lidar between 35 and 70 km, *Geophys. Res. Lett.*, **7**, 565–568, 1980.
- Hitchman, M. H., and C. B. Leovy, Diurnal tide in the equatorial middle atmosphere as seen in LIMS temperatures, *J. Atmos. Sci.*, **42**, 557–561, 1985.
- Hoxit, L. R., and R. M. Henry, Diurnal and annual temperature variations in the 30–60 km region as indicated by statistical analysis of rocketsonde data, *J. Atmos. Sci.*, **30**, 922–933, 1973.
- Kähler, M., The effects of non-linearity on thermal tides in a 3-D numerical model, *J. Atmos. Terr. Phys.*, **51**, 101–110, 1989a.
- Kähler, M., Nonclassical atmospheric tidal components in a 3-D model induced by a perturbation of the tropospheric heating, paper presented at 14th General Assembly, Eur. Geophys. Soc., Barcelona, March 1989b.
- Lindzen, R. S., and S. Chapman, Atmospheric tides, *Space Sci. Rev.*, **10**, 3–188, 1969.
- Manson, A. H., and C. E. Meek, Dynamics of the middle atmosphere at Saskatoon (52°N, 107°W): A spectral study during 1981, 1982, *J. Atmos. Terr. Phys.*, **48**, 1039–1055, 1986.
- Manson, A. H., C. E. Meek, S. K. Avery, and D. Tetenbaum, Comparison of mean wind and tidal fields at Saskatoon (52°N, 107°W) and Poker Flat (65°N, 147°W) during 1983/1984, *Phys. Scr.*, **37**, 169–177, 1988.
- Manson, A. H., C. E. Meek, H. Teitelbaum, F. Vial, R. Schminder, D. Kürschner, M. J. Smith, G. J. Fraser, and R. R. Clark, Climatologies of semi-diurnal and diurnal tides in the middle atmosphere (70–110 km) at middle latitudes (40–55°), *J. Atmos. Terr. Phys.*, **51**, 579–593, 1989.
- Mathews, J. D., J. K. Breakall, and G. K. Karawas, The discrete prolate spheroidal filter as a digital signal processing tool, *MAP Handb.* **9**, pp. 563–572, Univ. of Ill., Urbana, 1983.
- Press, W. H., B. P. Flannery, S. A. Teukolsky, and W. T. Vetterling, *Numerical Recipes*, 818 pp., Cambridge University Press, New York, 1986.
- Teitelbaum, H., Nonlinear interaction of tides and planetary waves, paper presented at 5th Scientific Assembly, Int. Assoc. of Meteorol. and Atmos. Phys., Reading, England, July–Aug. 1989.
- Tsuda, T., T. Nakamura, and S. Kato, Mean winds observed by the Kyoto meteor radar in 1983–1985, *J. Atmos. Terr. Phys.*, **49**, 461–466, 1987.
- Tsuda, T., S. Kato, A. H. Manson, and C. E. Meek, Characteristics of semidiurnal tides observed by the Kyoto meteor radar and Saskatoon medium-frequency radar, *J. Geophys. Res.*, **93**, 7027–7036, 1988.
- Vial, F., Numerical simulations of atmospheric tides for solstice conditions, *J. Geophys. Res.*, **91**, 8955–8969, 1986.
- Vial, F., Tides in the middle atmosphere, *J. Atmos. Terr. Phys.*, **51**, 3–17, 1989.
- Vincent, R. A., T. Tsuda, and S. Kato, A comparative study of mesospheric solar tides observed at Adelaide and Kyoto, *J. Geophys. Res.*, **93**, 699–708, 1988.
- Walterscheid, R. L., G. G. Sivjee, G. Schubert, and R. M. Hamway, Large-amplitude semidiurnal temperature variations in the polar mesopause: Evidence of a pseudotide, *Nature*, **324**, 347–349, 1986.
- Wilson, R., Climatologie des ondes de gravité dans l'atmosphère moyenne: Observation par lidar Rayleigh et interprétation, thesis, Univ. of Paris VI, 1989.

M.-L. Chanin and A. Hauchecorne, Service d'Aéronomie du Centre National de la Recherche Scientifique, B.P. 3, 91371 Verrières-le-Buisson Cédex, France.
S. T. Gille, 54-1421, Massachusetts Institute of Technology, Cambridge, MA 02139.

(Received August 16, 1990;
revised October 23, 1990;
accepted October 24, 1990.)